Accepted to Phys. Fluids 10.1063/5.0173510

Note on the startup of Couette flow for viscoelastic fluids

Corneliu Balan

Affiliation: N.U.S.T. Politehnica Bucharest, Hydraulics Depart., REOROM Laboratory, Splaiul Independentei 313, 060042 Bucharest, Romania.

Correspondence: corneliu.balan@upb.ro

Abstract

The paper is concerned with the numerical modelling of viscoelastic fluids in non-steady shear motions. The time dependent solutions for 3-constants differential models are obtained at the startup of the planar Couette flows. The influences of: (i) the Reynolds number, (ii) the value of κ − material parameter (the ratio between the retardation time and relaxation time), and (iii) the initial condition for the normal stress, on the velocity and stresses distributions in the gap are investigated using the numerical solutions obtained with *Mathematica* software. The focus of the study is the analysis of the Jaumann model (characterized by the corotational derivative) in transitory simple shear rheological tests, as function of initial conditions for stresses. The steady solutions, corroborated with the non-monotonicity of the steady flow curve, confirm the kink presence in the steady velocity distributions and the formation of shear bandings at $Re \geq 1$. The analyses of the strain- and stress-controlled simulations performed at different initial and boundary conditions offer possible explanations of some spurious data recorded in shear measurements of complex viscoelastic fluids. The findings have important consequences for performing transient shear experiments, specifically it is demonstrated that reproducibility and correlations between the tests require the control of initial normal stresses in the sample.

Accepted to Phys. Fluids 10.1063/5.0173510

1. Introduction

In this work we first introduce the well-known 3-constant differential models and briefly analyze their behavior in simple shear flow, in relation to the type of objective derivatives; this is followed by a discussion of the pioneering work of Tanner on transient start-up flow of a viscoelastic Oldroyd-B model (characterized by convective derivative). To extend Tanner's work, wherein a system of three partial differential equations collapses into one for the Oldroyd-B fluid, we numerically solve the full system of three equations (the equation of motion coupled with two constitutive equations) for the Jaumann (corotational) model. Different boundary conditions and parameters values are explored regarding their impacts on the time-space evolutions of the velocity and shear stress profiles in the Couette configuration. Especially for the Jaumann corotational model, the results demonstrate intriguing insights into the flow dynamics relating to material instability and shear banding formation. For the first time the dependencies of steady velocity and shear stress in the gap on the initial values of the normal stresses are highlight, result which may have important consequences in the analyzing and performing shear measurements in rotational rheometers.

The differential 3-constants models[1,2] for the extra-stress tensor $\mathbf{T}$ in a viscoelastic fluid have the generic expression,

$$\lambda_1 \frac{D\mathbf{T}}{Dt} + \mathbf{T} = 2\eta_0\lambda_2 \frac{D\mathbf{D}}{Dt} + 2\eta_0\mathbf{D} \tag{1}$$

where:

$$\frac{D*}{Dt} = \frac{d*}{dt} - \boldsymbol{\Omega} * + * \boldsymbol{\Omega} - a_i\,(\mathbf{D} * + * \mathbf{D}), \tag{2}$$

are the objective Gordon-Schowalter time derivatives[3-6] with $\mathbf{D}$ the strain rate tensor, $\boldsymbol{\Omega}$ the spin tensor and $\frac{d*}{dt}$ the material derivative. The material constants are: λ_1 – the relaxation time, λ_2 – the retardation time and η_0 – the viscosity coefficient.

The parameters $a_i \in [-1,\ 1]$ characterize the type of objective derivatives for the extra-stress and for the strain rate, respectively. The convected derivatives are defined for $a_i = \pm 1$ (Oldroyd models with constant steady viscosity), $a_i = 0$ defines the Jaumann (corotational) derivative and $-1 < a_i < 1$ was considered by Johnson and Segalman[7] for viscoelastic fluids with not affine deformation.

Different objective derivative in (1), a_1 for extra − stress and a_2 for strain rate tensors ($a_1 \neq a_2$), were proposed by Balan and Fosdick[8] (details in Annex A), who obtained for the isochoric viscometric flows the analytical solution of (1),

$$\begin{aligned}\mathbf{T}(t) = &\left\{e^{[\gamma(t)-\gamma(0)]\mathbf{A}}[\mathbf{T}(0) - 2\kappa\eta_0\mathbf{D}(0)]e^{[\gamma(t)-\gamma(0)]\mathbf{A}^T}\right\}e^{-\frac{t}{\lambda_1}} + 2\kappa\eta_0\mathbf{D}(t) + \\ &\frac{2\eta_0}{\lambda_1}(1-\kappa)\int_0^t\left\{e^{[\gamma(t)-\gamma(0)]\mathbf{A}}\mathbf{D}(s)e^{[\gamma(t)-\gamma(0)]\mathbf{A}^T}\right\}e^{-\frac{t-s}{\lambda_1}}ds \\ &+ 4\eta_0\kappa(a_1 - a_2)\int_0^t\left\{e^{[\gamma(t)-\gamma(0)]\mathbf{A}}\mathbf{D}^2(s)e^{[\gamma(t)-\gamma(0)]\mathbf{A}^T}\right\}e^{-\frac{t-s}{\lambda_1}}ds\end{aligned} \tag{3}$$

with $\mathbf{A} = \frac{1}{2}(1+a_1)\,\mathbf{e}_1\otimes\mathbf{e}_2 - \frac{1}{2}(1-a_1)\,\mathbf{e}_2\otimes\mathbf{e}_1$ and $\kappa = \lambda_2/\lambda_1$.

In (3) γ is the strain, with $\dot{\gamma} := \partial\gamma/\partial t = \sqrt{4|I_2|}$ the corresponding strain rate (or shear rate), where I_2 is the second invariant of $\mathbf{D}$.

The most important function in simple shear is the flow curve, i.e. the dependence of the shear stress σ as function of the shear rate $\dot{\gamma}$. The steady solution of (3) for the flow curve

$$\sigma(\dot{\gamma}) = \frac{1+\kappa(1-a^2)(\lambda\dot{\gamma})^2}{1+(1-a^2)(\lambda\dot{\gamma})^2}\eta_0\dot{\gamma}\,, \tag{4}$$

(where $\lambda_1 = \lambda$ and $a_1 = a_2 = a$), indicates that Oldroyd models $(a = \pm 1)$ have a steady constant viscosity, since the Jaumann model $(a = 0)$ discloses a shear thinning behavior. However, for $a = 0$ and $\kappa < 1/9$ the function (4) becomes non-monotonic, the viscosity function $\eta(\dot{\gamma}) := \sigma(\dot{\gamma})/\dot{\gamma}$ being identically in this case with the Carreau generalized Newtonian model[1-3] for a negative shear exponent ($n = -1$, respectively).

The validity of the constitutive relation for a viscoelastic fluid sample is established and confirmed in simple shear and extensional flows, modelled in rotational and capillary rheometers or in extensional devices.

The rotational rheometers generate non-stationary shear flows of the tested fluid located between two parallel surfaces (plate-plate, concentric cylinders) or cone-plate configuration. In the limit of small gaps, this dynamic might be considered a simple shear flow, i.e. the planar one-dimensional impulsive Couette flow between two infinite plates, Fig. 1. The solution to this problem for a viscoelastic fluid is not trivial since the equation of motion has to be coupled with the constitutive relation for the stresses[9], in particular with the set of four differential equations corresponding to (1).

Accepted to Phys. Fluids 10.1063/5.0173510

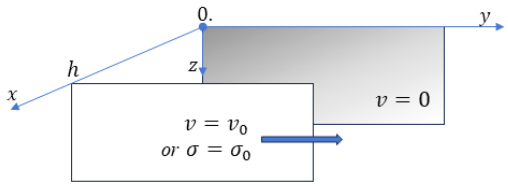

Fig.1. Simple shear Couette flow between two infinite parallel plates with one directional velocity distribution $v_y = v(x,t), v_x = v_z = 0$, and boundary conditions for the lower plate – $v = 0$ at $x = 0$, and for the upper plate – $v = v_0$ or $\sigma = \sigma_0$ at $x = h$, where v_0 and σ_0 (the shear stress) are constant values. Adherence condition of the fluid at the walls is assumed.

The starting point of the studies dedicated to the impulsive shear flows is the exact analytic solution of the Rayleigh-Stokes first problem for a pure viscous fluid[9,10]: the flow generated in an infinite viscous fluid (initially at rest) by an infinite planar plate put suddenly in motion with constant one directional velocity. This solution was later extended for steady/oscillatory imposed velocity at the boundaries of the Couette configuration[11].

To my knowledge, the first numerical solution of the Rayleigh-Stokes problem for a viscoelastic fluid was obtained by Roger Tanner (probably in his PhD thesis, Manchester University, 1961) and published in 1962[12]. For a simple shear of the viscoelastic fluid (1), the final PDEs system in non-dimensional form is given by a set of three equations[13],

$$Re\frac{\partial v}{\partial t} = \frac{\partial \sigma}{\partial x} \tag{5}$$

$$\frac{\partial N}{\partial t} + N = 2(1-a^2)\left[\sigma\frac{\partial v}{\partial x} - \kappa\left(\frac{\partial v}{\partial x}\right)^2\right] \tag{6}$$

$$\frac{\partial \sigma}{\partial t} + \sigma = \kappa\frac{\partial^2 v}{\partial x \partial t} - \left(\frac{N}{2} - 1\right)\frac{\partial v}{\partial x} \tag{7}$$

with three unknowns: (i) velocity - $v(x,t)$, (ii) shear stress - $\sigma(x,t)$, (iii) normal stress - $N(x,t)$ and two parameters: κ and a. Relation (5) is the equation of motion and (6)-(7) correspond to the constitutive relation (1), with the local shear rate: $\dot{\gamma} = \partial v/\partial x$ (see Annex A).

In (5)-(7) $Re = \rho v_0 h/\eta_0$ is the Reynolds number and the reference quantities: $v_0, h, \lambda_1, \eta_0/\lambda_1$ are used for velocity, space, time, and stresses, respectively. Without to lose the generality, the Deborah number ($De = \lambda_1 v_o/h$) is considered here equal to unity. In (6) and (7) $N = (1-a)N_1 - 2aN_2$ represents the contribution of the normal stresses, N_1 and N_2 being the first and the second normal stresses differences[1].

Roger Tanner obtained in the 1962 paper[12] the solution for the Oldroyd-B model, $a = 1$ in (2). In this case, from (6) results $N \sim f(x)e^{-t}$, with $f(x) = 0$ for zero initial condition of the normal stresses difference N_2. Therefore, the system (5)-(7) is resumed to one single 3-order PDE,

$$Re\left(\frac{\partial^2 v}{\partial t^2} + \frac{\partial v}{\partial t}\right) = \kappa \frac{\partial^3 v}{\partial x^2 \partial t} + \frac{\partial^2 v}{\partial x^2} \qquad (8)$$

with the velocity unknown. I mention here that Tanner used for the reference space scale the dimension $\sqrt{\frac{\eta_0 \lambda_1}{\rho}}$, therefore $Re = 1$ in (8).

The author analyzed in this paper the influence of $\kappa -$ parameter on the solution of (8) and represents the time dependence of velocity at constant x, from $\kappa = 0$ (damped wave equation, Maxwell fluid) to $\kappa = 1$ (diffusion equation, Newtonian fluid). The numerical solutions for $0 < \kappa < 1$ are discussed in relation to the asymptotic limit solutions and the impact of the stored elastic energy on the transitory flow regime.

Analyses of $\kappa -$ parameter's influence on the solutions for the viscoelastic Rayleigh-Stokes problem were later reconsidered by Huilgol[14] and Phan-Thien&Chew[15], the methods to obtain the analytic solutions being reviewed by Renardy[16] et. al.

Analytic viscoelastic solutions for the Oldroyd-B model[16-22] (or for the first and second order fluids[23-25]) were also obtained for different planar configurations and boundary conditions, but without to investigate explicitly the influence of the Reynolds number (most of the solutions being obtained in the limit $Re \to 0$).

In the present paper numerical solutions of the system (5)-(7) are calculated with the *Wolfram Mathematica* 13.2 software for the boundary and initial conditions corresponding to the startup motion of the Couette flow. The setting of the controlled parameters, in relation to the convergence and precision of solutions, and the influences of the initial/boundary conditions are analyses in Annex B.

The goal of the study is to investigate the influences of parameters *Re*, κ, a and boundary/initial conditions on the time-space variations of the velocity and shear stress in the gap. The results evidence some interesting insights of the flow dynamics, especially for the corotational model ($a = 0$) in relation to the material instability and shear banding formation.

2. Results and Discussions

2.1 Startup of Couette flows at constant boundary velocities

The PDEs system (5)-(7) is solved in the domain $x \in [0, \bar{x}]$ and $t \in [0, 10)$, for the unknown functions: $v(x,t), \sigma(x,t)$ and $N(x,t)$, with boundary/initial conditions for velocities:

$$\text{(i) } v(\bar{x},t) = v_0 = 1, \text{ (ii) } v(0,t) = 0, \text{ (iii) } v(x,0) = v_0 \cdot \mathrm{H}[x - \bar{x}], \tag{9}$$

and the initial conditions for the stresses:

$$\text{(iv) } \sigma(x,0) = \sigma_0 = 0, \text{ (v) } N(x,0) = N_0, \tag{10}$$

at constant imposed values of Re, a and κ.

2.2 Couette flow in a large gap

The Rayleigh-Stokes first problem is the impulsive flow in a semi-infinite space domain, i.e. $x \in [0, \infty)$, with $v(0,t) = v_0$, $v(\infty, t) = 0$ and zero initial stresses (where $x = 0$ indicates the position of the plate). Since numerical solutions are obtained in a finite space domain, one considers in this paper a large gap, $\bar{x} = 100$, $Re = 1$ and the associated boundary conditions (9)-(10) with $N_0 = 0$. The numerical solutions shown in Fig. 2 are good approximations in the vicinity of the moving plate of the analytic solutions for the Newtonian[10,11] and Oldroyd-B[12] fluids, respectively (see Annex B.1).

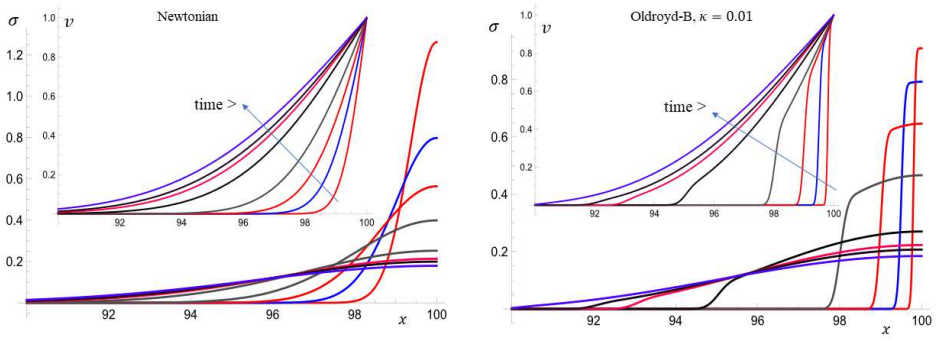

Fig. 2. Space variation of the Newtonian and Oldroyd-B solutions for shear stress and velocity, at constant times ($t = 0.2, 0.5, 1, 5, 7, 8, 10$), in the vicinity of the moving plate, $90 < x \leq 100$, at $Re = 1$ and $v(100, t) = 1$.

Not relevant qualitative differences between the Newtonian (pure viscous fluid) and the Oldroyd-B solutions are observed as κ is decreasing from 1 (Newtonian case) to 0.1. Major differences appear at lower values of κ, $\kappa \ll 1$, as can be observed in Figs. 2-4. The results from Fig. 3.a,b and Fig. 4 are similar with the velocity distributions presented by Tanner[12]:

(i) solutions at $\kappa = 0.2$ and $\kappa = 0.4$ are consistent with the results from Tanner's paper[12], (as is shown in Fig. B.1), (ii) the solutions at $\kappa \leq 0.001$ disclose the elastic wave generated in the domain with velocity $c = \sqrt{\frac{\eta_0}{\rho\lambda_1}}$ (the speed of the vortex sheet propagation[14]).

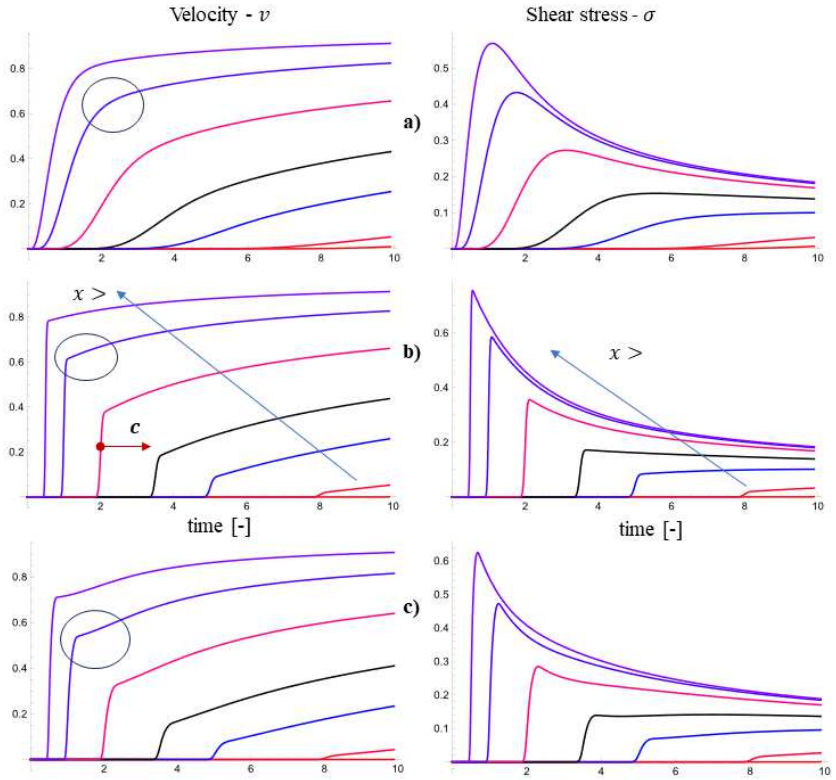

Fig. 3. Time variations of velocity and shear stress at constant distance from the moving plate ($x = 92, 95, 96.5, 98, 99, 99.5$) at the onset of the flow, $t < 10$, $Re = 1$ and $v(100, t) = 1$: a) Oldroyd-B ($a = 1$), $\kappa = 0.2$; b) Oldroyd-B ($a = 1$), $\kappa = 0.001$; c) Jaumann ($a = 0$), $\kappa = 0.001$.

For $\kappa \ll 1$ the velocity $v(x, t)$ has a sharp increasing at $t = t^*$ and $x = x^* = constant$, for both the Oldroyd-B and Jaumann models, Fig. 4 (where $t = t_c$ is the time which corresponds to $\partial^2 v(x, t)/\partial t^2 = 0$). This result indicates the presence of the elastic wave. The difference between the two models is observable in the vicinity of t_c, $t > t_c$, where a non-monotonic tendency of $\partial v(x^*, t)/\partial t$ for the Jaumann's model is remarked, see the marked regions from

Fig. 3. The constant speed $c = 1$ at $Re = 1$ for the elastic wave and the exponential distribution of velocity at $t = 10$ from Fig. 4.b,c are results confirmed by previous published solutions[12,14,15].

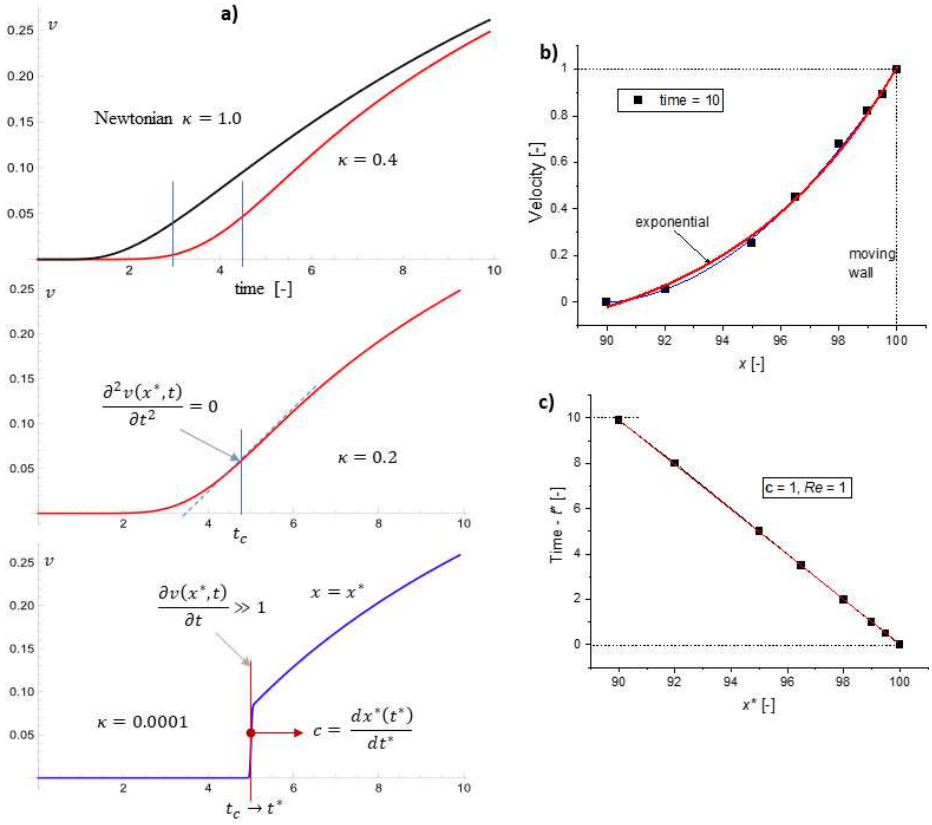

Fig. 4. (a) Influence of κ-coefficient on the velocity distribution at $x^*= 95$ for $a = 1$ and $Re =1$. Here t_c is the time corresponding to the change in curvature and c is the wave speed of the vortex sheet propagation (at the limit $\kappa \to 0$); (b) velocity distribution $v(x^*, 10)$, (c) dependence $t^*(x^*)$, $x \in [90 \div 100]$, at $\kappa = 0.001$.

One concludes that our solutions in large finite gaps are fair approximations of the analytic and numerical solutions for the Newtonian and Oldroyd-B fluids in the vicinity of the moving plate, at the startup of the Rayleigh-Stokes flow. Also, the simulations confirm the elastic wave propagation in the flow domain for $\kappa \ll 1$. The effect of elasticity and normal stresses are investigated in more details in the next paragraph, where solutions of the transitory Couette flows in finite geometry are analyzed.

2.3 Couette flow in a simple shear configuration

The time dependent planar Couette flow in the domain $x \in [0,1]$, $\bar{x} = 1$ in (9), is a good approximation of the simple shear flow generated in rotational rheometers corresponding to the boundary conditions (9), an experiment assumed to be performed at an apparent constant shear rate, $\dot{\gamma}_c = 1$ at $v_0 = 1$. The time dependence of velocity between the two plates is present for any fluid models, but at $Re << 1$ the steady state (represented by the linear velocity distribution) is considered in rheometry to be reached almost instantaneously, with a constant shear rate in the gap. In this case the equation (5) is neglected, and the dynamics is reduced to the time dependence of the stresses. Once the *Re*-number approach unity inertia becomes important and the corrections of the measured data in rheometry are needed[26,27].

Solutions of the system (5)-(7), with conditions (9)-(10) and $N_0 = 0$, disclose for $Re > 0.1$ oscillations of velocity and a longer time to achieve steady state for viscoelastic models in comparison to the Newtonian case, as is shown in Fig. 5 and Fig. 6.

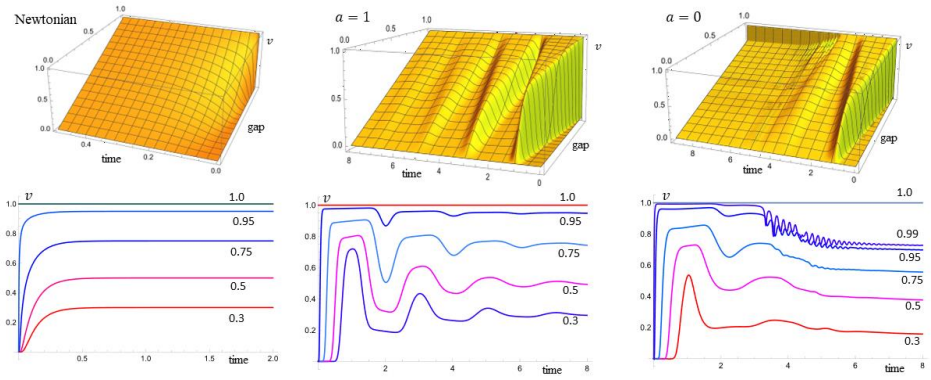

Fig. 5. Velocity distribution $v(x,t)$ in the gap (Re = 1 and $v(1,t) = v_0 = 1$) for Newtonian, Oldroyd ($a = 1$, $\kappa = 0.01$) and Jaumann ($a = 0, \kappa = 0.01$) fluids, at some constant values of $x \in (0,1]$.

We remark that steady state for $a = 1$ is independent on the *Re*-number, the steady shear rate and the corresponding shear stress being constants in the gap. At $a = 0$ the steady velocity distribution discloses for $Re \geq 1$ a kink (i.e. discontinuity in the velocity derivative) in the vicinity of the moving wall, the steady shear stress is maintained constant in the gap but is decreasing with the increasing of *Re*-number (Fig. 6).

Accepted to Phys. Fluids 10.1063/5.0173510

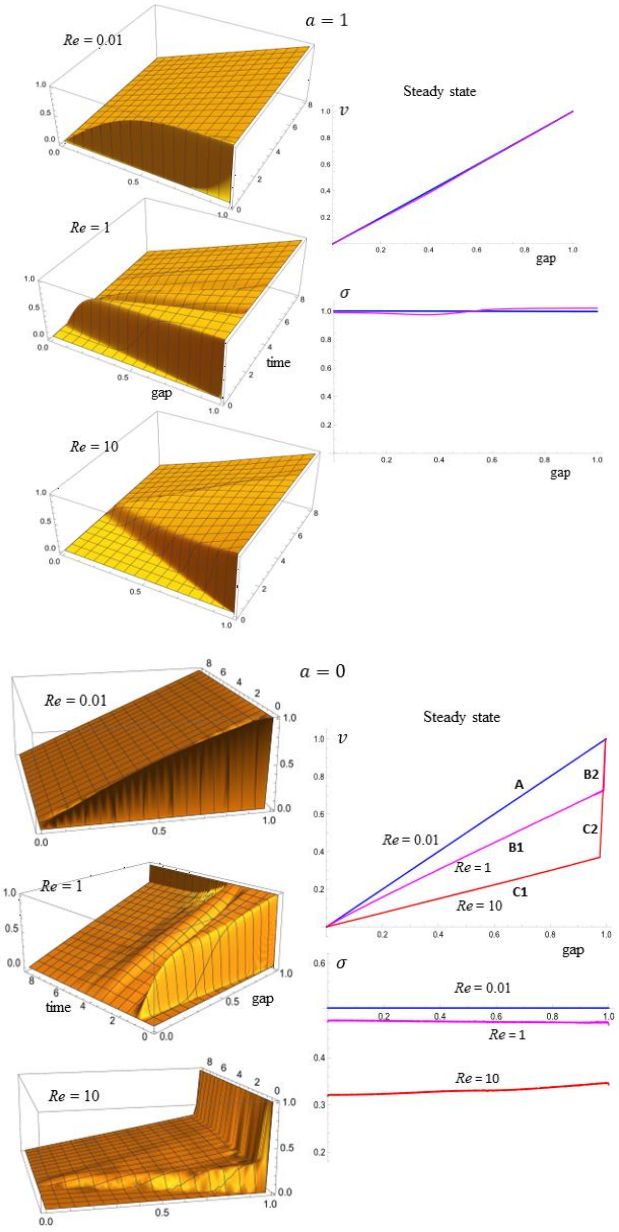

Fig. 6. Dependence of the velocity distribution $v(x,t)$ in the gap ($v(1,t) = v_0 = 1,\ \kappa = 0.01$) as function of the *Re*-number; comparison between the Oldroyd fluid ($a = 1$) and the Jaumann fluid ($a = 0$).

The dynamic of the Jaumann model is a direct consequence of the non-monotonic steady flow curve and the existence of the instability region $\sigma_{min} \leq \sigma_0 \leq \sigma_{max}$, as is depicted in Fig. 7, where two distinctive values of the steady shear rates coexist at same value σ_0. The influence of the non-monotonic steady flow curves on the flow instability[28-31] and shear banding formation[32-39] were investigated in numerous papers in the last decades; is still a topic of interest in rheology, but not a subject for the present work. However, our results are connected to these topics since shear banding is associated with the discontinuity of the shear rate in the gap, therefore with the presence of at least one kink in the velocity distribution.

Numerical solutions of PDEs system (with well posed boundary and initial conditions) are dependent of the numerical scheme, the space mesh, and the time step size. In Annex B.2 the influences of some setting parameters in *Mathematica* code are investigated. We found that the value of *MaxStepSize* (maximum time step size) is the most influential on the convergence and precision of the results (in our case the time distribution in the gap of velocity and stresses). We concluded that for *MaxStepSize* ≤ 0.001 the solutions are convergent, and precision is satisfactory. The final steady results in the interval $0.0002 \leq MaxStepSize \leq 0.001$ do not differ qualitatively, the quantitative difference being below 1%, e.g. $\sigma_0 \cong 0.478$ at $MaxStepSize = 0.001$ and $\sigma_0 \cong 0.482$ at $MaxStepSize = 0.0002$ for $v_0 = 1$.

The simulations shown in the present paper were performed with the following parameters: *InitialStepSize* = 0.0001, *MaxStepSize* = 0.001 (or 0.0005). The confidence in results is also supported by the very good match of the final steady solutions of (5)-(7) with the steady flow curve (4), Fig. 7. The marked areas in Fig. 7 indicate the domains of possible variations of the steady values of shear stress and shear rate, which depend on the computation precision, i.e. on the imposed value of *MaxStepSize* ≤ 0.001, and implicit on the number of grid points (fixed automatically by *Mathematica* to minimize/control the error in a given time interval).

Accepted to Phys. Fluids 10.1063/5.0173510

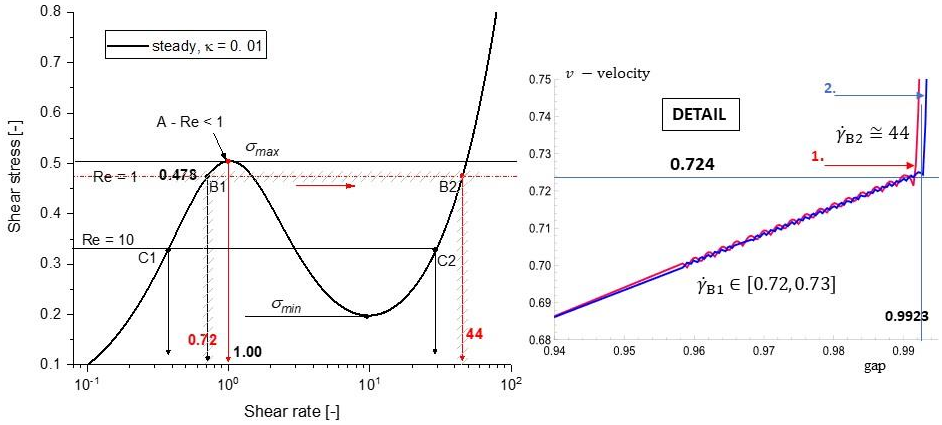

Fig. 7. Non-monotonic steady state flow curve $\sigma(\dot{\gamma})$ of the Jaumann model, relation (4) with $a = 0$ and $\kappa = 0.01$; for $Re \geq 1$ two shear rates coexist at the same value of the shear stress, see Fig. 6. At $Re = 1$ the jump from B1 to B2 takes place at $\sigma = \sigma_0 \cong 0.478$; value which determines the plateau in the flow curve from $\dot{\gamma}_1 \cong 0.72$ to $\dot{\gamma}_2 \cong 44$. In the detail are shown two solutions of the velocity distributions in the vicinity of the kink (1 – *MaxStepSize* = 0.001, 2 – *MaxStepSize* = 0.0002); oscillations with very small amplitudes (less 0.03%, however they are increasing with the increasing of the step size) are recorded before the kink.

The evolutions in the gap of the unknown time-dependent functions from (5)-(7) at $Re = 1$ are represented in Fig. 8. As *Re*-number is increasing, $Re \geq 1$, the position of the jump in shear rates is moved to lower values of shear stress, Fig.7. At $Re < 1$ the jump takes place in point A, the maximum of the first stable branch. The jump in shear rate at constant shear stress determines sometimes called the "plateau region" of the shear stress σ_0. At $\sigma = \sigma_0$ corresponds 3 steady solutions: B1/C1 are nodes, B2/C2 are foci, both being stable, with the middle unstable saddle solution (detailed analysis of this dynamics at $Re = 0$ is presented by Balan[13]).

The steady flow curve depends on the values of κ and the positions of the jump (and implicit the value of the shear stress σ_0) is determined not only by *Re*-number, but also by the imposed boundary and initial conditions (subject investigated in the next paragraph). For three values of κ, the steady flow curves, velocity and shear stress in the gap are represented at $Re = 1$ in Fig. 9.

Accepted to Phys. Fluids 10.1063/5.0173510

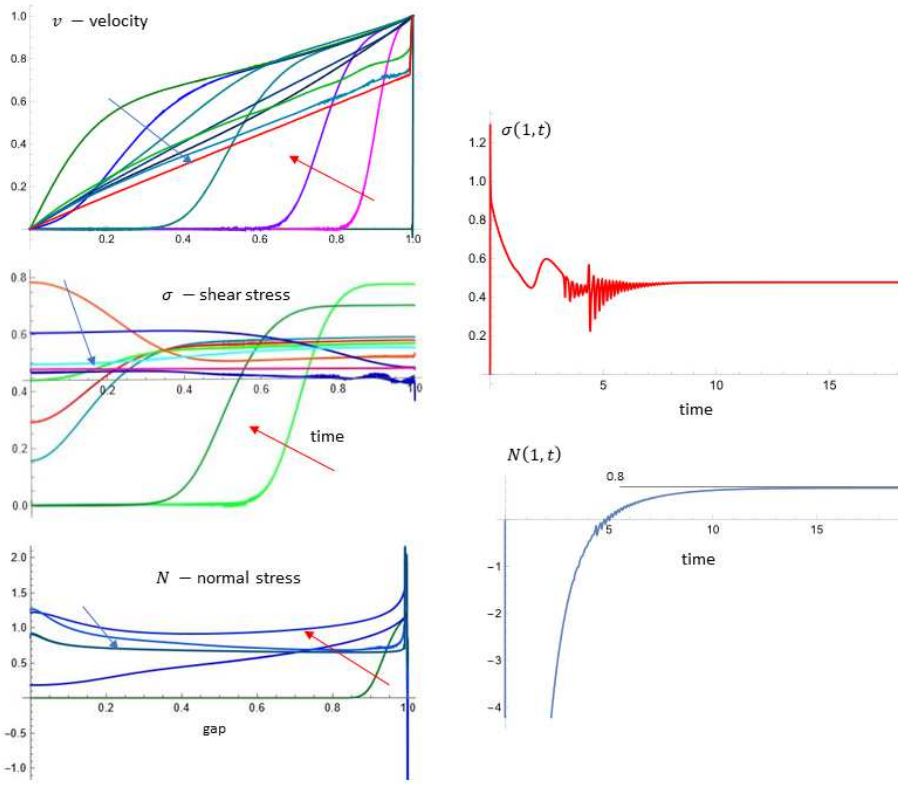

Fig. 8. Time variations in the gap of the solutions for velocity, shear stress and normal stress with time as parameter ($a = 0, \kappa = 0.01$; $Re = 1$). The time dependence of shear stress σ and normal stress N at the moving plate with $v(1,t) = v_0 = 1, \sigma(x,0) = 0,\ N(x,0) = 0$, are also represented.

At shear rate one, for $\kappa = 0.1$ the velocity distribution is linear, since the corresponding value of the shear stress, $\sigma = 0.55$, has a unique intersection with the flow curve. As κ is decreasing there are two stable solutions for the shear rate, therefore the kink is present in the velocity distribution. For very low values of κ ($\kappa = 0.001$ in Fig. 9) the area of instability (associated with the influence of initial conditions to the steady state) is increasing (marked on the graph), the steady shear stress disclose oscillations in the gap and the velocity has kinks in the vicinity of the plates. The jump of the shear rate in the gap at constant shear stress determines the formation of one or two shear bands, which in our simulations are represented by thin layers attached to the plates.

Accepted to Phys. Fluids 10.1063/5.0173510

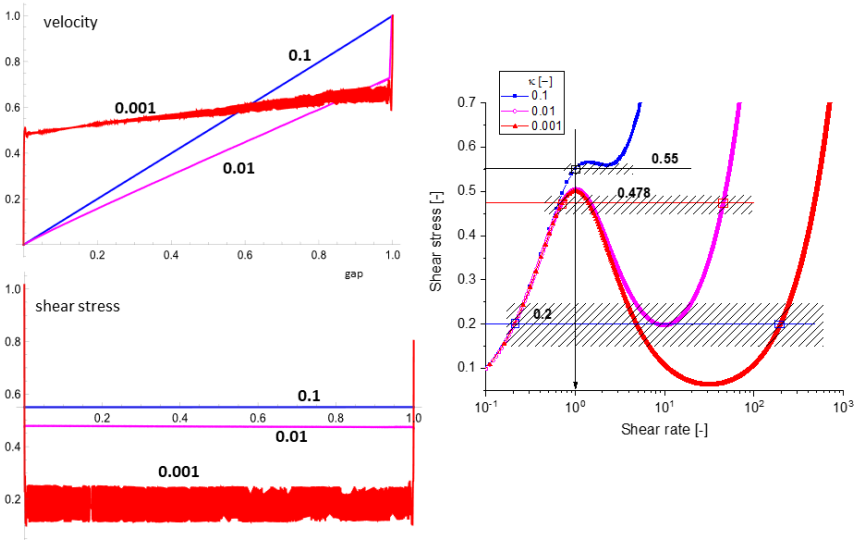

Fig. 9. Steady flow curves and the corresponding steady distributions of the velocity and shear stress in the gap at $\kappa = 0.1; 0.01; 0.001$ ($a = 0$, $Re = 1$; $v(1,t) = v_0 = 1$, $\sigma(x,0) = 0$, $N(x,0) = 0$).

Similar results are obtained for any model with non-monotonic steady flow curve, in the presence or in the absence of elasticity[40-47]. Increasing instability (i.e. the jump takes place at a lower value of σ_0 than expected) due to random perturbations induced by the end-effects or modified boundary conditions are also observed[48]. The experiments and direct visualizations of the steady velocity distributions confirm the present simulations[49-56].

In conclusion, the dynamics of the analyzed Couette viscoelastic flows, under constant imposed velocities at the plates (so called in rheometry the strain-controlled test) and zero initial stresses in the gap, are dependent on three parameters: (i) a-parameter, which gives the type of the objective derivative, (ii) κ-coefficient, the ratio between the retardation time and the relaxation time, (iii) the value of the Reynolds number.

3. Startup of Couette flows: the influences of boundary and initial conditions

The previous analysis[13] of the system (5)-(7) for $a = 0$ at $Re = 0$ and constant shear stresses located in the unstable region proved that basin of attraction for the steady solutions is determined by the initial values of the normal stresses, Fig. 10.a (see also Fig. 7). Therefore, at one constant value σ_0 two steady solutions for the steady shear rate might coexisting, which indicates a jump between the stable branches of the flow curve, e.g. at $\sigma_0 = 0.45$ the jump takes place for $N_0 \geq 1.4$; at $\sigma_0 = 0.5$ the jump from A1 (the maximum of the first stable branch) to A2 is obtained for $N_0 \geq 1.183$, Fig. 10.b. Of course, the transitory regimes are different for A1 and A2, the time dependence of the shear rate discloses high oscillations for the A2 solution, which are not observed for A1 solution (time-parametric plots $\dot{\gamma}(N)$ and $\sigma(N)$ are also represented in Figs.10). In constant shear stress mode (called creeping if $Re \to 0$) the initial shear rate is always zero at the beginning of the rheological test ($\dot{\gamma}(0) = \dot{\gamma}_0 = 0$), but the control of the initial normal stresses is difficult in experiments due to initial squeezing of the visco-elasto-plastic samples in the gap of the rheometer before any rheological test performed in plate-plate or cone-plate configurations (it is important to remark that normal force is set automatically to zero by the software of the rheometer at the onset of the measurements).

One concludes that dynamics of constitutive relation with non-monotonic steady flow curve (the Jaumann model in our case) discloses in creeping at least one bifurcation point (sensitive to the initial conditions). If simulations are performed at constant shear rate (strain-controlled experiment) the steady shear stress values are unique and some solutions are obtained on the unstable branch of the flow curve, which are not reached in the stress-controlled mode, Fig. 10.a. In steady state, at $Re = 0$, the shear stress and shear rate have constant values in the gap and the velocity distributions are linear (however, they are dependent on the initial value of N_0).

The coexisting in the gap of the two values for the steady shear rate is possible for the Jaumann model only if $Re > 0$; in this case the velocity distribution has at least one kink (as was shown in the previous paragraph). The same result was obtained in the absence of elasticity, for the generalized Newtonian fluids with non-monotonic flow curve, i.e. Carreau model with negative exponent[47].

Accepted to Phys. Fluids 10.1063/5.0173510

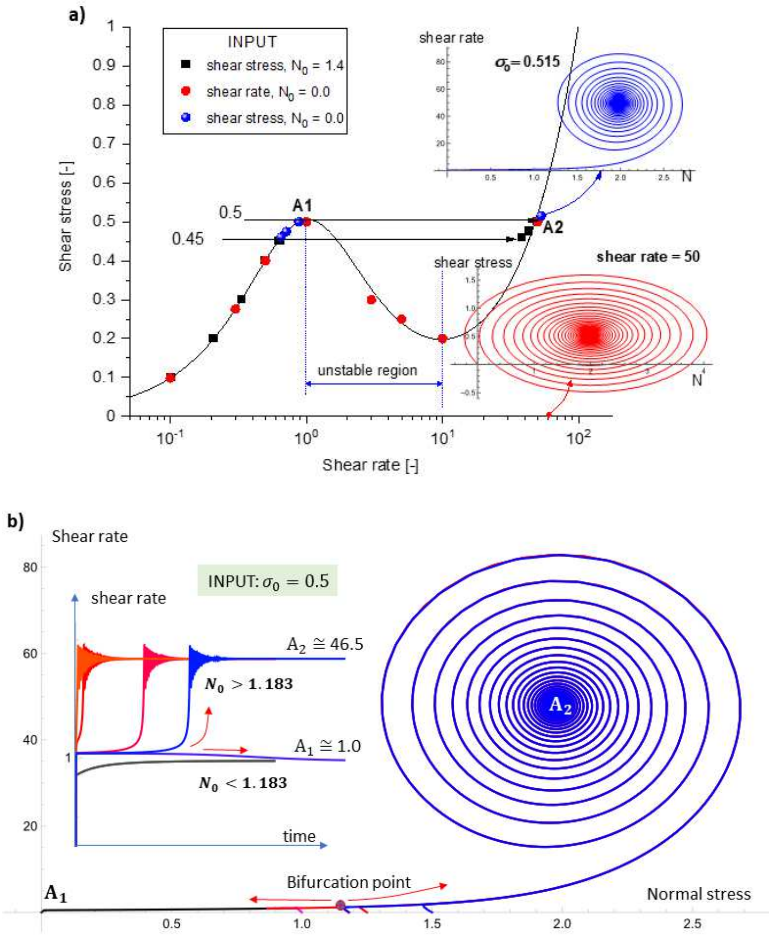

Fig. 10. (a) Steady flow curve $\sigma(\dot{\gamma})$ of the Jaumann model ($a = 0, \kappa = 0.01$); time-parametric plots: $\dot{\gamma}(N)$ at $\sigma_0 = 0.515$ and $\sigma(N)$ at $\dot{\gamma} = 50$, with $N_0 = 0$, are also represented at $Re = 0$. (b) Dynamics $\dot{\gamma}(N)$ at constant applied shear stress $\sigma_0 = 0.5$ and different initial conditions for the normal stress; the solutions A1 and A2 coexist at the same value of the shear stress for different initial normal stress, see the time dependences of the shear rate $\dot{\gamma}(t)$.

The influences of the initial value of the normal stress $N_0 = N(x, 0)$ at $Re = 1$ are shown in Fig. 11. For the Oldroyd model ($a = 1$) the influence of N_0 is mainly observed during the transitory variation of the shear stress in the gap, which becomes wavy at high N_0 values until reach the same unique steady state independently on N_0.

Accepted to Phys. Fluids 10.1063/5.0173510

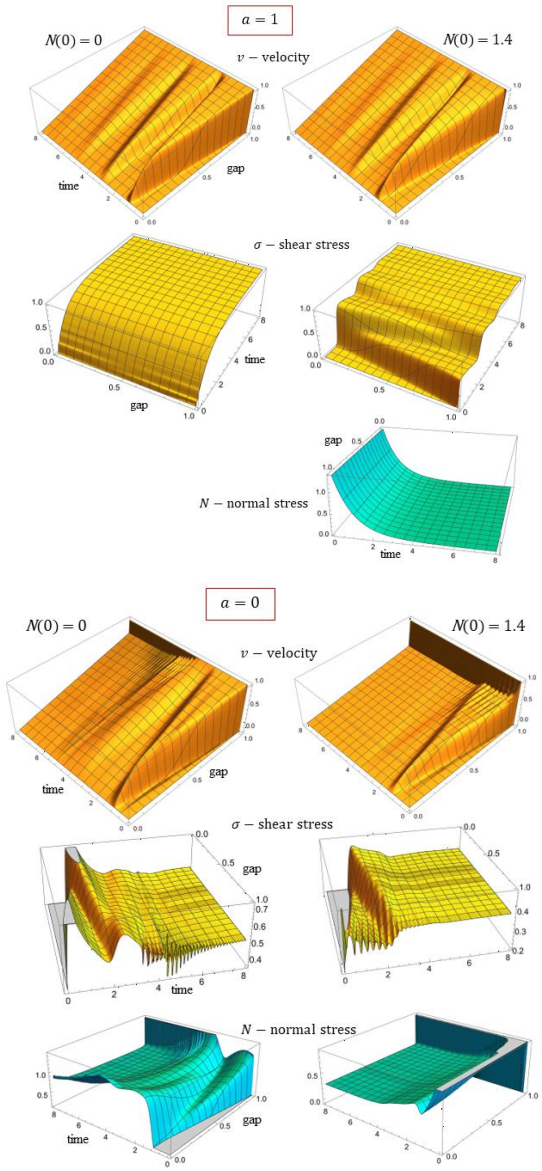

Fig. 11. The influence of the initial conditions for the normal stress N on the dynamics of the motion in the gap for $a = 1$ and $a = 0$ ($Re = 1$, $\kappa = 0.01$, strain-controlled test). The steady state in Oldroyd model is independent of the initial value of the normal stress, while the Jaumann model is sensitive to those values, even though the kink in the steady velocity distribution is always present.

The Jaumann model ($a = 0$) reaches faster the steady state with increasing of N_0, but at lower steady value of the shear stress than for $N_0 = 0$, and as consequence the steady velocity distribution is quantitatively different, the kink being located at lower values of velocity, Fig. 11 (details in Annex B.2). During the transitory regime, the velocity oscillates in the gap for all viscoelastic models; in Fig. 12 the instantaneous velocities at instant $t = 2$ are shown for two initial values of N_0.

It is important to mention that at $Re > 0$ and constant initial shear rate in the gap, i.e. $v(x, 0) = v_0 \cdot x$ (linear velocity distribution at $t = 0$), the steady state is not dependent on the normal stress N_0 and numerical solutions are not stable if the initial shear rate corresponds to the unstable branch of the steady flow curve from Fig. 10.a. However, this strain-controlled test is just hypothetical, being impossible to be implemented in reality (even though it is considered in rheometry as an approximation of the Couette flow in the limit of $Re \to 0$).

Until now, the solutions at $Re > 0$ were obtained for constant applied velocities at the plates (strain-controlled experiment) with boundary conditions (9). Numerical simulations have been also performed imposing a constant value for the shear stress at the moving boundary: $\sigma_0 = \sigma(1, t)$, and keeping the adherence conditions of the fluid at the plates, so called the stress-controlled experiment (we mention that rotational rheometer controls the applied torque, which is related for each test geometry with corresponding shear stress[1,2]). A comparison between stress-controlled and strain-controlled simulations is shown in Fig. 13. If the input is $\sigma_0 > \sigma_{max}$ (or $\sigma_0 < \sigma_{min}$), a single value for the shear stress corresponds to one of the stable branch of the flow curve (see Fig. 7); therefore, a steady linear velocity distribution is obtained in the gap (and a constant shear rate), with the value $v_0 = v(1, t)$ of velocity at the moving plate. This velocity is later used in the strain-controlled test, where the same steady constant value of the shear stress σ_0 is finally obtained in the gap. It is important to mention that a steady state for the stress-controlled simulation is reached after a longer time in comparison with the strain controlled one. In this case the application between the steady values on the moving plate is bijective for the two tests, the final steady states being independent on the type of boundary conditions and initial values of normal stress.

If $\sigma_{min} \leq \sigma_0 \leq \sigma_{max}$, i.e. the imposed value of the shear stress is in the region of instability, the steady results are sensitive to the initial conditions for the normal stress N_0. This statement is proved by the comparison of the simulations from Fig. 14 and Fig. 15, both at $Re = 1$. The controlled stress experiment at $\sigma_0 = 0.478$ generates different steady velocities at the moving plate: $v_0 = 0.72$ (linear velocity distribution) and $v_0 = 4.2$ (velocity distribution with a kink) for different values of the initial normal stress. The corresponding strain-controlled tests are shown in Fig. 15. Only the steady velocity distribution for the input data: $v_0 = 0.72$ and $N_0 = 0$ gives an identical result with the corresponding stress-controlled experiment, the other velocities distributions being different. We remark the presence of two kinks in vicinity of the plates for $v_0 = 4.2$ and $N_0 = 0.0$.

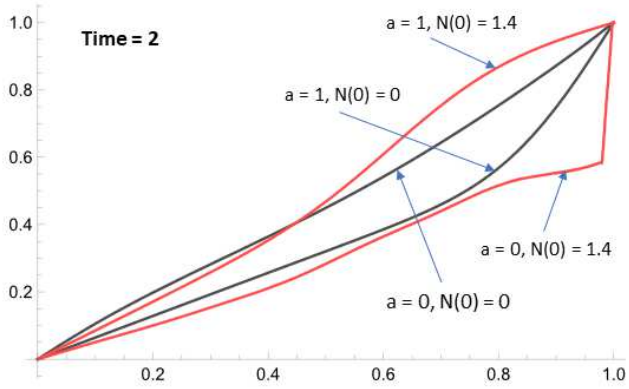

Fig. 12. Velocity distributions at $t = 2$ and $Re = 1$ for two initial values of the normal stress (details from Fig. 11). At this instant the kink if formed only for $N_0 = 1.4$.

Accepted to Phys. Fluids 10.1063/5.0173510

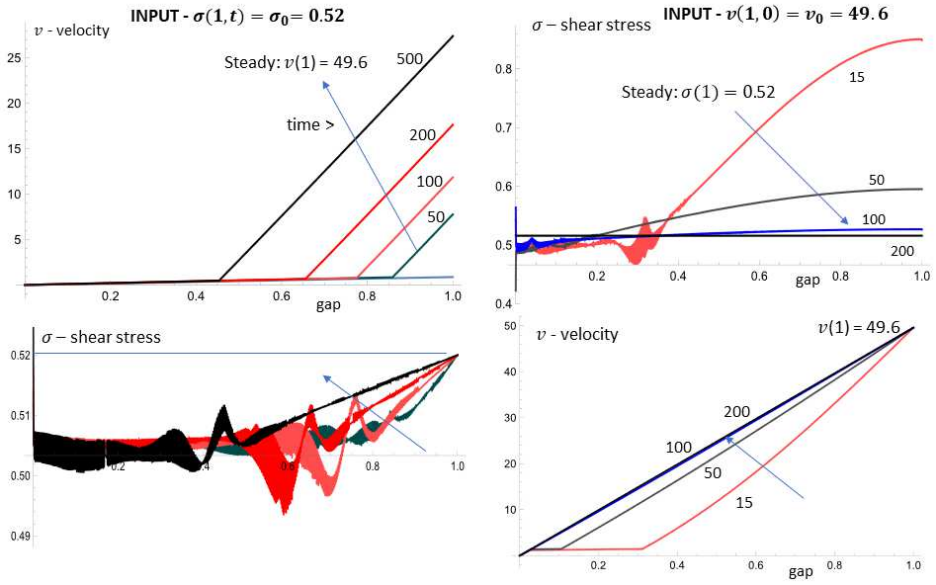

Fig. 13. Shear stress and velocity variations in the gap at constant values of time (controlled stress and controlled strain tests for the Jaumann model at $\sigma_0 > \sigma_{max}$, $Re = 1$, $\kappa = 0.01, N_0 = 0$). During the transitory regime the shear stress discloses oscillations in both experiments, but the final steady state is the same.

Accepted to Phys. Fluids 10.1063/5.0173510

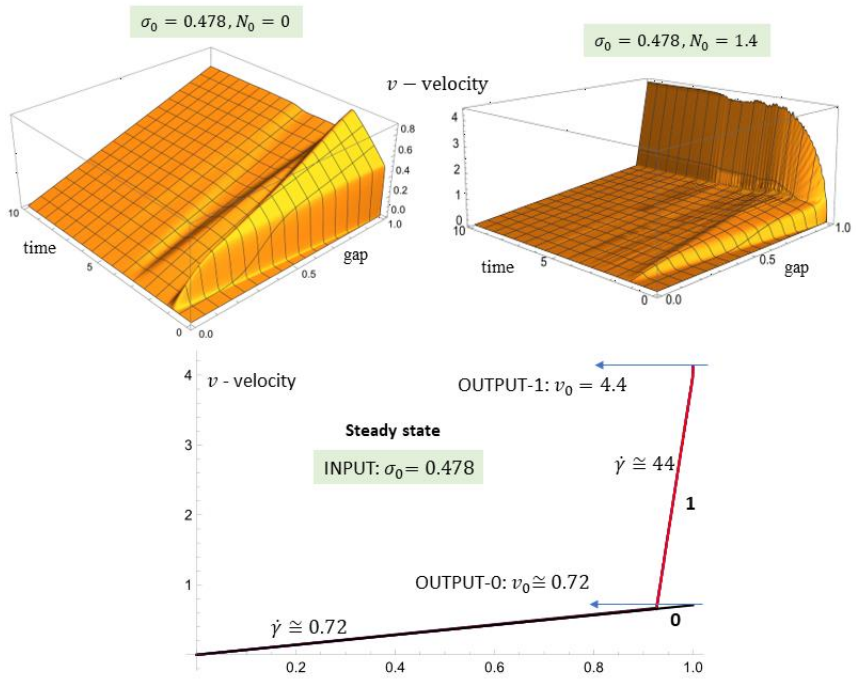

Fig. 14. Velocity distributions in the stress-controlled experiment (marked with "0" for $N_0 = 0$ and with "1" for $N_0 = 1.4$) at $\sigma_0 = 0.475$ ($Re = 1, a = 0, \kappa = 0.01$).

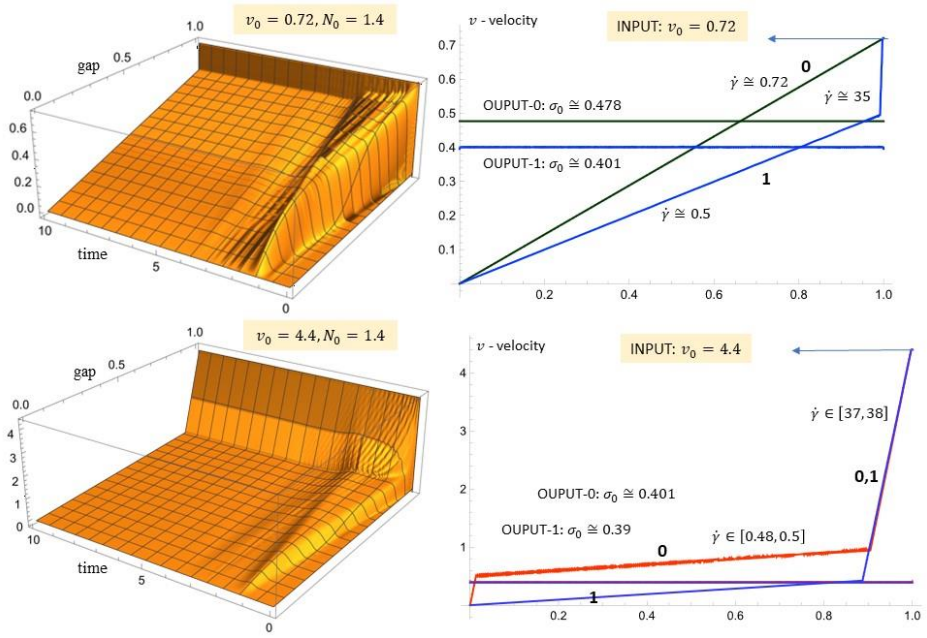

Fig. 15. Velocity distributions in the strain-controlled experiment (marked with "0" for $N_0 = 0$ and with "1" for $N_0 = 1.4$) at two input values of velocity: $v_0 = 0.72$ and $v_0 = 4.44$, respectively ($Re = 1$, $a = 0$, $\kappa = 0.01$).

One concludes that initial value of normal stress, $N_0 > 0$, has a significant influence during the transitory motion and determines the final steady values of the shear rate and stresses.

The present simulations prove that viscoelastic fluids embedded in some internal network structure, samples included in the category of *soft solids* (as gels, creams/greases, dense suspensions) may produce confusing results during their characterization in shear flows. The apparent lack of correlation between strain- and stress-controlled tests is usually related with the slip of the sample at solid surface. This might be not the only cause of wall depletion, since is difficult to distinguish the real slip from the existence of a thin shear band of sample in the very vicinity of the wall [30,31,42,47]. If the measurements are interpreted in the framework of constitutive relations with non-monotonic flow curves, keeping valid the hypothesis of wall adherence, the data possibly indicate the material instability of the sample in the range of tested shear rates and shear stresses. In this case we have to admit that two or three shear rates coexist in the gap under the same shear stress.

Accepted to Phys. Fluids 10.1063/5.0173510

4. Final remarks and conclusions

The paper was focused on the analysis of numerical solutions for 3-constants differential viscoelastic models in transient planar Couette flow, as function of the Re-number and the material parameter κ (the ratio between the retardation and relaxation times). The main aim was to investigate the effect of boundary and initial conditions on the time dependent velocity distributions in the gap for the Jaumann model (corotational derivative), in comparison to the Oldroyd model (convected derivative).

The non-monotonicity of the steady flow curve generates in the case of the Jaumann model the presence of kinks in velocity distribution, their existence and location being dependent on the Re-number and the initial values for normal stresses (at constant $\kappa -$ parameter). The numerical findings are consistent with previous theoretical and experimental results published in literature and offer the possibility to investigate in more detail the instability phenomena and shear banding formation, which are observed in the flows of some complex fluids.

One main conclusion of the work is the importance of the initial normal stresses in the rheometry of fluids which are subject to material instability and/or spurious phenomena[57-59]. The control of squeezing force in plate-plate or cone-plate configurations becomes necessary at the beginning of rheological tests to avoid possible confusions between real and apparent slipping (or shear banding formations) of the samples during the shear experiments [37,38,54,59,60].

The modelling and analysis of unsteady simple shear/elongational flows of viscoelastic/complex fluids are the theoretical background of applied rheology. The startup of Couette flow between two parallel plates is a fair approximation for the dynamics of simple shear flows used in rotational rheometry. The validation of the solutions for viscoelastic/plastic models in this configuration using the experimental data is compulsory to establish the proper constitutive relation for the samples under investigation.

From a historical perspective[61], Tanner's paper[12] had a great impact in rheology, revealing the importance of the analytic and numeric time dependent viscoelastic solutions for developing the measurement techniques. The analysis and modelling of transient tests in stress/strain-controlled modes, in shear and elongational motions, are indispensable for a complete rheological characterization of complex fluids.

Accepted to Phys. Fluids 10.1063/5.0173510

Since my PhD period spent at TU Darmstadt (1990-1991), I have a constant interest in modelling viscoelastic fluids in transitory flows and Roger's paper[12] was one of the first I studied, a reference work for me. Most probably, I wouldn't submitted to a journal a paper on startup of Couette flow if Physics of Fluids would not be dedicated a special issue to Professor Roger Tanner.

I met Roger a couple of times in Cambridge and in Wales; I was never close to him, but I still remember a short dialogue with Roger in Liverpool, at the British Society Meeting dedicated to Complex Flows of Complex Fluids in March 2008. It was during an evening visit of the participants at the Merseyside Maritime Museum; I took the opportunity to give then my appreciation to Roger for the 1962 paper.
He was smiling:

" *… is nice for me to hear that somebody is still interested in my old work, but do not take too seriously the papers published at the beginning of the scientist's carrier …*"

My answer (in playful mode): *I always took your paper seriously*; *I am interested to read the first published papers of great scientists …*
He touched gently with the hand my shoulder, keeping the smile on his face …

"… let's go for the dinner, my young colleague".

Last time we crossed the eyes at Portmeirion in 2011, at the 20th anniversary of Institute of Non-Newtonian Fluids from Wales.

This paper is dedicated to Professor Roger Tanner. Tanner's viscoelastic solutions for the Rayleigh problem published in 1962 was a value pioneering work in applying numerical computations in viscoelasticity and had a major contribution in a better understanding of fluids elasticity in transitory motions.

Supplementary Material

Two Annexes are attached to the paper as supplement material:

(i) **ANNEX A – Non-dimensional PDEs system** contains the justification of using different objective derivatives in the constitutive relation (1) and the procedure to obtain its equivalent PDEs system for a simple shear flow in non-dimensional form, relations (6)-(7), respectively.
(ii) **ANNEX B – PDEs solutions with *Mathemtica* software** presents details of using the numerical code. There are 2 sections in which the numerical results are analyzed:
   1) B1. Comparison with Tanner solutions.
   2) B2. Startup of Couette flow for the Jaumann viscoelastic model,
      B.2.1 Influences of the values for StartingStepSize, MaxStepSize and PlotPoints,
      B.2.2 Influence of boundary conditions,
      B.2.3 Influence of initial value for the normal stress.

Accepted to Phys. Fluids 10.1063/5.0173510

Conflict of Interest Statement
The author has no conflicts to disclose.

Data availability
The data that support the findings of this study are available within the article.

Acknowledgement
The author acknowledges the financial support of CHIST-ERA – 19 – XAI – 009 MUCCA project, by the founding of EC and The Romania Executive Agency for Higher Education, Research, Development, and Innovation Funding - UEFISCDI, grant COFUND-CHIST-ERA no. 206/2019.

The recommendations and suggestions of the referees improved the quality of the manuscript; I acknowledge their contributions to the final version of the paper.

References
[1]H. A. Barnes, J. F. Hutton and K. Walters, *An introduction to rheology* (Elsevier, 1989).
[2]R.I.Tanner, *Engineering rheology* (Oxford Univ. Press, 2000).
[3]R. G. Larson, *The structure and rheology of complex fluids* (Oxford Univ. Press, 1999).
[4]W. R. Schowalter, *Mechanics of non-Newtonian fluids* (Pergamon Press, 1978).
[5]H. Giesekus, *Phänomenologische Rheologie* (Springer, 1994).
[6]G. Böhme, *Strömungsmechanik nichtnewtonscher Fluide* (B.G. Teubner, 2000).
[7]M. Johnson and D. Segalman, "A model for the viscoelastic fluid behavior which allows non-affine deformations," J. Non-Newtonian Fluid Mech., **2**, 255 – 270 (1977).
[8]C. Balan and R. Fosdick, "Constitutive relation with coexisting strain rates," Int. J. Non-Linear Mech., **35**, 1023 – 1043 (2000).
[9]R. B. Bird, R. C. Armstrong and O. Hassager, *Dynamics of polymeric liquids – vol. 1* (Wiley, 1977).
[10]H. Lamb, *Hydrodynamics* (Dover Publ., 1945).
[11]H. Schlichting, *Boundary layer theory* (Pergamon Press, 1955).
[12]R. I. Tanner," Note on the Rayleigh problem for a visco-elastic fluid," Z. angew. Math. Phys. **13**, 573-580 (1962).
[13]C. Balan, "Experimental and numerical investigations on the pure material instability of an Oldroyd's 3-constant model," Continuum. Mech. Thermodyn., **13**, 399 – 414 (2001).
[14]R. R. Huilgol,"Propagation of the vortex sheet in viscoelastic liquids – the Rayleigh problem,", J. Non-Newtonian Fluid Mech. 8, 337-347 (1981).
[15]N. Phan-Thien and Y.T. Chew, "On the Rayleigh problem for viscoelastic fluid," J. Non-Newtonian Fluid Mech. **28**, 117-127 (1988).
[16]M. Renardy, W. J. Hrusa and J. A. Nohel, *Mathematical problems in viscoelasticity* (Longman 1987).
[17] K. R. Rajagopal and R. K. Bhatnagar, "Exact solutions for some simple flows of an Oldroyd-B fluid," Acta Mech. **113**, 233 (1995).
[18]T. Hayat, A. M. Siddiqui, and S. Asghar, "Some simple flows of an Oldroyd-B fluid," Int. J. Eng. Sci. **39**, 135 (2001).
[19]N. Aksel, C. Fetecau and M. Scholle, "Starting solutions for some unsteady unidirectional flows of Oldroyd-B fluids," Z. angew. Math. Phys. **57**, 815-831 (2006).

[20]C. Fetecau1,T. Hayat, M. Khan and C. Fetecau, "Unsteady flow of an Oldroyd-B fluid induced by the impulsive motion of a plate between two side walls perpendicular to the plate," Acta Mech **198**, 21–33 (2008).
[21]W. Tan and T. Masuoka, "Stokes' first problem for an Oldroyd-B fluid in a porous half space, Phys. Fluids **17**, 023101 (2005).
[22]N. Shahid1, M. Rana and I. Siddique, "Exact solution for motion of an Oldroyd-B fluid over an infinite flat plate that applies an oscillating shear stress to the fluid," Boundary Value Problems **48**, (2012).
[23]R. I. Tanner, "Plane creeping flow of incompressible second order fluids," Phys. of Fluids **9**, 1246-1247 (1966).
[24]K. R. Rajagopal, "A note on unsteady unidirectional flows of a non-Newtonian fluid," Int. J. Non-Linear Mech. **17**, 369-373 (1982).
[25]J. S. Vrentas and C. M. Vrentas,"Unsteady flows of first-order fluids, "Ind. Eng. Chem. Res. **34**, 3203-3207 (1995).
[26]K. Walters, *Rheometry* (Chapman and Hall, 1975).
[27]Ch. M. Macosko, *Rheology: Principles, Measurements, and Applications* (Wiley - WCM, 1994).
[28]R. W. Kolkka, D. S. Malkus, M. G. Hansen and G. R. Ierley, "Spurt phenomena of the Johnson-Segalman fluid and related models," J. Non-Newtonian Fluid Mech. **29**, 303–335 (1988).
[29]D. S. Malkus, J. A. Nohel, and B. J. Plohr, "Dynamics of shear flow of a non-Newtonian fluid," J. Comp. Phys. **87**, 464–487 (1990).
[30]R. G. Larson, "Instabilities in viscoelastic flows," Rheol. Acta **31**, 213 – 263 (1992).
[31]M. A. Fardin, T. Divoux, M. A. Guedeau-Boudeville, I. Buchet-Maulien, J. Browaeys, G. H. McKinley, S. Manneville, and S. Lerouge, "Shear-banding in surfactant wormlike micelles: Elastic instabilities and wall slip," Soft Matter **8**, 2535–2553 (2012).
[32] N. A. Spenley, X. F. Yuan, and M. E. Cates, "Nonmonotonic constitutive laws and the formation of shear-banded flows," J. Physique, **6**, 551-571 (1996).
[33]P. Español, X. F. Yuan, and R. C. Ball, "Shear banding flow in the Johnson-Segalman fluid," J. Non-Newtonian Fluid Mech., 65, 93-109 (1996).
[34]S. M. Fielding, "Complex dynamics of shear banded flows," Soft Matter, **3**, 1262–1279 (2007).
[35]P. D. Olmsted,"Perspectives on shear banding in complex fluids," Rheol. Acta, **47**, 283-300 (2008).
[36]G. Ovarlez, S. Rodts, X. Chateau and P. Coussot, "Phenomenology and physical origin of shear-localization and shear-banding in complex fluids," Rheol. Acta 48, 831-844 (2009).
[37]T. Divoux, M. A. Fardin, S. Manneville, and S. Lerouge, "Shear banding of complex fluids," Annu. Rev. Fluid Mech. **48**, 81–103 (2016).
[38]M. A. Fardin, T. J. Ober, G. C. Gregoire, G. H. McKinley, and S. Lerouge, "Potential ''ways of thinking'' about the shear-banding phenomenon," Soft Matter, **8**, 910-922 (2012).
[39]E. J. Hemingway and S. M. Fielding, S. M. (2020). "Interplay of edge fracture and shear banding in complex fluids," J. Rheol. **64**, 1147 (2020).
[40]P. D. Olmsted and P. M. Goldbard, "Isotropic-nematic transtion in shear flow: State selection, coexistence, phase transitions, and critical behaviour," Phys. Rev. A, **46**, 4966-4993 (1992).
[41]F. Greco and R. C. Ball, "Shear-band formation in a non-Newtonian fluid model with a constitutive instability," J. Non-Newtonian Fluid Mech., **69**, 195–206 (1997).
[42]J. M. Adams, S. M. Fielding, and P.D. Olmsted, "The interplay between boundary conditions and flow geometries in shear banding: Hysteresis, band configurations, and surface transitions," J. Non-Newtonian Fluid Mech., **151**, 101-118 (2008).
[43]F. Bautista, J. F. A. Soltero, J. H. Petez-Lopez, J. E. Puig, and O. Manero, "On the shear banding flow of elongated micellar solutions," J. Non-Newtonian Fluid Mech., **94**, 57–66 (2000).

[44]P. R. de Souza Mendes and R. L. Thompson, "A unified approach to model elasto-viscoplastic thixotropic yield-stress materials and apparent-yield-stress fluids," Rheol Acta, **52**, 673-694 (2013).
[45]R. L. Moorcroft and S. M. Fielding, „Shear banding in time-dependent flows of polymeris and wormlike micelles," J. Rheol., **58**, 103-147 (2014)
[46]L. Zhou, G. H. McKinley and L. P. Cook, "Wormlike micellar solutions: III. VCM model predictions in steady and transient shearing flows" J. Non-Newtonian Fluid Mech. **211**. 70–83 (2014).
[47]D. Broboana, C. S. Ionescu and C. Balan, "Numerical modeling of shear banding formation in rheometry," *11th Int. Symp. ATEE,* Bucharest, 1-6 (2019).
[48] C. Balan and J. M. Franco, "Influence of the geometry on the transient and steady flow of lubricating greases," Tribology Transaction, **44**, 53 – 58 (2001).
[49] M. M. Britton, R. W. Mair, R. K. Lambert and P. T. Callaghan, "Transition to shear banding in pipe and Couette flow of wormlike micellar solutions," J. Rheol., **43**, 897–909 (1999).
[50]L. Becu, S. Manneville and A. Colin, "Spatio temporal dynamics of wormlike micelles under shear, " Phys. Rev. Lett. **93**, 018301(2004).
[51] D. Broboana and C. Balan,"Investigations of rheology of water-in-crude oil emulsions," U.P.B. Sci. Bull. B **69**, 35-50 (2007).
[52]P. E. Boukany and S. Q. Wang, "Use of particle-tracking velocimetry and flow birefringence to study nonlinear flow behavior of entangled wormlike micellar solution: from wall slip, bulk disentanglement to chain scission," Macromolecules **41**, 1455-1464 (2008).
[53]D. Bonn, S. Rodts, M. Groenink, S. Rafaï, N. Shahidzadeh-Bonn, and P. Coussot, "Some applications of magnetic resonance imaging in fluid mechanics: complex flows and complex fluids." Annu. Rev. Fluid Mech. **40**, 209–233 (2008).
[54]M. P. Lettinga and S. Manneville, "Competition between shear banding and wall slip in wormlike micelles." Phys. Rev. Lett. **103**, 248302 (2009).
[55] R. Buscall, T. Kusuma, A. Stickland, S. Rubasingha, P. Scales, H-E Teo, and G. Worrall, "The non-monotonic shear-thinning flow of two strongly cohesive concentrated suspensions," J. Non-Newtonain Fluid Mech. **222**, 112-120 (2015).
[56]H. Perrin, C. Clavaud, M. Wyart, B. Metzger and Y. Forterre, "Interparticle friction leads to nonmonotonic flow curves and hysteresis in viscous suspensions", Phys. Rev. X. **9**, 10.1103 (2019).
[57]W.B. Black and M. D. Graham, "Wall-slip and polymer-melt flow instability," Phys. Rev. Lett. **77**, 956-959 (1996).
[58] D. Coblas, D. Broboana and C. Balan, "Correlation between large amplitude oscillatory shear (LAOS) and steady shear of soft solids at the onset of the fluid rheological behavior," Polymer **104**, 215-226 (2016).
[59]Barnes, H. A., "A review of the slip (wall depletion) of polymer solutions, emulsions and particle suspensions in viscometers: its cause, character and cure," J. Non-Newtonian Fluid Mech. **56**, 221–251(1995).
[60]S. Lerouge, "Flow of wormlike micelles: From shear banding to elastic turbulence", Science Talks **3**, 100050 (2022).
[61]R.I. Tanner and K. Walters (edit.), *Rheology: An historical perspective* (Elsevier, 1998).